The Astrophysical Journal Letters, 894:L11 (7pp), 2020 May 1 https://doi.org/10.3847/2041-8213/ab8795

Solar-type Stars Observed by LAMOST and Kepler

Jinghua Zhang[1], Alexander I. Shapiro[2], Shaolan Bi[1], Maosheng Xiang[3], Timo Reinhold[2], Krishnamurthy Sowmya[2], Yaguang Li[4], Tanda Li[5], Jie Yu[2], Minghao Du[1], and Xianfei Zhang[1]
[1] Department of Astronomy, Beijing Normal University, Beijing 100875, People's Republic of China; zhangjinghua@mail.bnu.edu.cn, bisl@bnu.edu.cn
[2] Max Planck Institute for Solar System Research, Göttingen, D-37077, Germany; shapiroa@mps.mpg.de
[3] Max Planck Institute for Astronomy, Königstuhl 17, D-69117, Heidelberg, Germany
[4] Sydney Institute for Astronomy (SIfA), School of Physics, University of Sydney, NSW 2006, Australia
[5] School of Physics and Astronomy, University of Birmingham, Edgbaston, Birmingham B15 2TT, UK
Received 2020 March 16; revised 2020 April 6; accepted 2020 April 6; published 2020 May 4

Abstract

Obtaining measurements of chromospheric and photometric activity of stars with near-solar fundamental parameters and rotation periods is important for a better understanding of solar–stellar connection. We select a sample of 2603 stars with near-solar fundamental parameters from the Large Sky Area Multi-Object Fiber Spectroscopic Telescope (LAMOST)-Kepler field and use LAMOST spectra to measure their chromospheric activity and Kepler light curves to measure their photospheric activity (i.e., the amplitude of the photometric variability). While the rotation periods of 1556 of these stars could not be measured due to the low amplitude of the photometric variability and highly irregular temporal profile of light curves, 254 stars were further identified as having near-solar rotation periods. We show that stars with near-solar rotation periods have chromospheric activities that are systematically higher than stars with undetected rotation periods. Furthermore, while the solar level of photospheric and chromospheric activity appears to be typical for stars with undetected rotation periods, the Sun appears to be less active than most stars with near-solar rotation periods (both in terms of photospheric and chromospheric activity).

Unified Astronomy Thesaurus concepts: Stellar activity (1580); Stellar photometry (1620); Stellar rotation (1629); Stellar spectral lines (1630); Solar activity (1475)

1. Introduction

The action of a dynamo generates magnetic field in the stellar interior (Charbonneau 2010, 2013). This field emerges in the stellar atmosphere leading to various manifestations of magnetic activity, e.g., brightness and spectroscopic variability, chromospheric, and coronal emission. The interest in stellar magnetic activity has been recently brought to a new level by the advent of high-precision transit photometry and subsequent discovery of thousands of exoplanets. This is particularly due to stellar magnetic activity appearing to be a limiting factor in exoplanet detection and characterization, and due to its possible influence on exoplanet atmospheres (see, e.g., Wood 2004; Vidotto 2019).

Among the most typical proxies of stellar magnetic activity are chromospheric Ca II *H* and *K* line emission (see, e.g., Noyes et al. 1984; Baliunas et al. 1995; Hall et al. 2007, and references therein) and amplitude of the photometric brightness variations (Basri et al. 2013; Reinhold et al. 2017). During the past few decades, the long-term synoptic HK projects at Mount Wilson Observatory (MWO; Wilson 1978) and at the Lowell Observatory (Hall et al. 2007) have been dedicated to measuring the Ca II *H* and *K* emission in late-type stars. Contemporary to monitoring of the stellar Ca II activity, Lowell and Fairborn Observatories initiated programs for measuring photometric variability of Sun-like stars (Radick et al. 1998, 2018; Lockwood et al. 2007; Hall et al. 2009). Interestingly, it was found that stars with near-solar level of chromospheric activity appear to be much more photometrically variable than the Sun on the decadal timescale. Several explanations of such a puzzle have been proposed; e.g., Witzke et al. (2018) suggested that the Sun corresponds to a local minimum of the complex dependence of the amplitude of brightness variations on the activity cycle timescale on fundamental stellar parameters and magnetic activity level.

While the MWO, Lowell, and Fairborn observations formed the backbone of stellar activity studies, they were limited to just a few hundreds of stars. The high-precision photometry from space telescopes, particularly from the Kepler mission that observed almost two hundred thousands of stars, allowed to circumvent this limitation. Also, the studies aimed at the comparison of solar and stellar variability enjoyed a breath of fresh air. In one of the first solar–stellar comparison studies based on the Kepler data, Gilliland et al. (2011) suggested that the Sun is photometrically quieter than other presumably main sequence Kepler stars with near-solar effective temperatures. Conversely, Basri et al. (2013) found that photometric variability of the Sun is similar to the level of variability displayed by the majority of Kepler stars with near-solar effective temperatures. Salabert et al. (2016) identified a sample of 18 solar analogs and found that their photometric variability and chromospheric activities are similar to those of the Sun.

Recently, Reinhold et al. (2020) combined Gaia and Kepler data to identify a sample of Kepler stars with effective temperatures between 5500 and 6000 K. 369 of these stars had rotation periods between 20 and 30 days, while rotation periods of 2529 stars could not be determined from the photometry. The photometric variability of the stars with non-detected periods appeared to be very similar to that of the Sun. This is not surprising, because the highly irregular temporal profile of solar brightness variations would make the detection of the solar rotation period from the photometric time-series very difficult (see, e.g., Aigrain et al. 2015; Witzke et al. 2020, and references therein). Consequently, if the Sun were observed by Kepler it would most probably be attributed to a sample of stars

with near-solar fundamental parameters but undetected rotation periods. Interestingly, Reinhold et al. (2020) found that despite having near-solar fundamental parameters and rotation periods, 369 stars with known rotation periods are significantly more variable than the Sun (e.g., the mean variability of the stars with detected periods is almost 5 times larger than solar median variability). Currently, the high variability of these stars and a regular pattern of their light curves remain unexplained. One of the important questions is whether there is any systematic difference between Ca II H and K emission of the stars with non-detected rotation periods and the Sun on one side and stars with detected near-solar rotation periods on the other side. This question is addressed in this Letter utilizing data from the Large Sky Area Multi-Object Fiber Spectroscopic Telescope (LAMOST) spectroscopic survey (Cui et al. 2012; Zhao et al. 2012).

LAMOST has collected millions of stellar spectra with a mean spectral resolution of about 1800 in broad wavelength range of 3700–9100 Å (Zhao et al. 2012). In particular, it provides vast amounts of Ca II H and K observational data. Meanwhile, LAMOST spectra allowed accurate determination of stellar fundamental parameters, i.e., effective temperature $T_{\rm eff}$, surface gravity $\log g$, and metallicity [Fe/H]. LAMOST has performed spectroscopic follow-up for targets in the Kepler field of view, which was initiated as the LAMOST-Kepler project (LK-project; De Cat et al. 2015). By 2017 June, this project obtained more than 227,000 low-resolution spectra (Zong et al. 2018), thus providing us with a tool required to answer the question raised above.

In this Letter, we select solar-type stars observed by both LAMOST and Kepler, and study the relation between period detectability and chromospheric activity. In Section 2, we explain the sample selection and the procedure for measuring the Ca II H and K emission from the LAMOST spectra. In Section 3, we compare the Ca II H and K emission of the Sun and stars with known and unknown rotation periods. We summarize our results in Section 4.

2. Data and Methods

2.1. Stellar Samples

The stars analyzed in this study have been selected from the sixth Data Release (DR6) of the LAMOST survey.[6] Here, we define solar-type stars as stars with $T_{\rm eff}$, $\log g$ and [Fe/H] in the ranges 5500–6000 K, 4.14–4.74, and −0.2–0.2, respectively. All these parameters are taken from DR6 of the LAMOST survey, which is based on the LAMOST stellar parameter pipeline (Zhao et al. 2012; Luo et al. 2015). The solar values were taken to be: $T_{\rm eff} = 5777$ K and $\log g = 4.44$. To place a lower limit on the quality of the spectroscopic observations, we only considered stars with the signal-to-noise ratios (S/Ns) at the blue end of the spectra higher than 30. With these constraints, we collected 341,557 spectra for 272,854 solar-type stars, which we denote as LAMOST sample. Among them, there are 6626 stars that have been also observed by Kepler mission (Zong et al. 2018), which we denote as the L-K sample.

We cross-matched the selected 6626 stars with the catalog of McQuillan et al. (2014). This is a catalog of Kepler stars containing 34,030 stars with detected rotation periods and 99,000 stars with non-detected rotation periods. Following Reinhold et al. (2020) we concentrated on stars with rotation periods in the range 20–30 days (hereafter, solar-type stars) and stars with non-detected rotation period (hereafter, non-periodic sample). Furthermore, we have also selected stars with periods in the range 10–20 days (hereafter, short-periodic sample). Such a classification results in 254 solar-type stars and 793 short-periodic stars; 1556 stars were deemed as non-periodic. These stars can be considered as pseudo solar-type stars because their rotation periods are unknown. As discussed in Section 1 the Sun would most probably be allocated to the non-periodic sample of pseudo solar-type stars. In the Appendix we also consider stars with rotation periods shorter than 10 days to better illustrate the effect of the rotation period on photometric variability and on Ca II H and K emission.

2.2. Chromospheric Activity

Using the LAMOST spectra, we measured the magnetic activity proxy S-index as

$$S_{\rm LAMOST} = \alpha \cdot \frac{H + K}{R + V}, \quad (1)$$

where H and K are the integrated fluxes in the cores of Ca II H and K lines, respectively. The integration is performed using a triangle function with a FWHM of 1.09 Å centered at 3968 Å and 3934 Å, respectively. The parameters R and V are the integrated fluxes in the nearby pseudo-continuum. The integration in pseudo-continuum is performed using a rectangular function with 20 Å width centered at 4001 Å and 3901 Å, respectively. Following Karoff et al. (2016) we put calibration factor α to 14.4. Karoff et al. (2016) argued that such a choice of the calibration factor leads to a distribution of LAMOST S-index values being consistent with that derived from Isaacson & Fischer (2010) around $S = 0.2$. For stars with multiple observations, the S-indexes were determined by using the weighted mean values of these multiple spectra with the weights being the S/Ns of the spectra. We refer to Zhang et al. (2020) for a detailed discussion of S-index measurements.

One of the main limitations of the current study is that Kepler and LAMOST observations are not performed at the same moment in time. While Kepler data considered in this study were obtained from 2009 June until 2013 May, most of the LAMOST spectra were taken from 2012 to 2017 June. Consequently, 92% of LAMOST spectra used in this study have been taken outside of the period of Kepler observations. Nevertheless, we do not expect S-index to change significantly between the periods of Kepler and LAMOST observations. Indeed, the amplitude of the S-index variability on the rotation and activity cycle timescales is proportional to the time-averaged values of the S-index (see, e.g., Egeland 2017; Radick et al. 2018, and references therein). Consequently, the changes of S-index values of stars in the solar-type and non-periodic samples are expected to be similar to those of the Sun (i.e., about 10% from the mean value). Furthermore, spectra of 577 stars in our samples have been recorded by LAMOST more than once with the intervals among observations often reaching a couple of years. Comparison of these spectra did not reveal any significant changes of the corresponding S-index values with time (e.g., standard deviation among S-index values for the majority of the non-periodic stars was below 0.01–0.015).

[6] http://dr6.lamost.org/

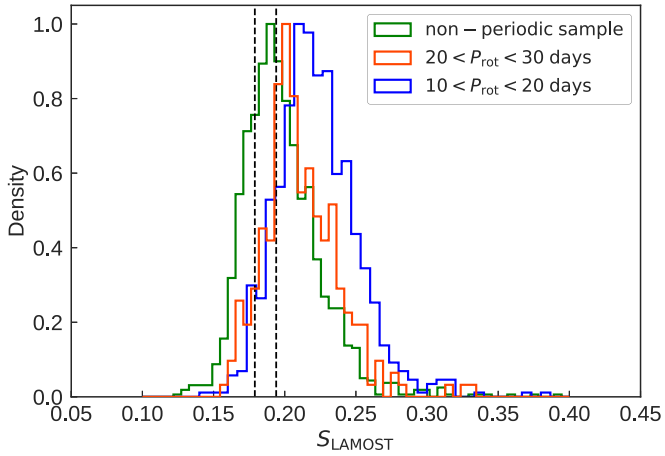

Figure 1. Distributions of the *S*-index values for the short-periodic sample (blue), solar-type sample (red), and non-periodic sample (green). The dashed vertical lines indicate the minimum and maximum values of the solar *S*-index as it would be measured by LAMOST during activity cycles 15–24 (see Section 3.3 for a detailed explanation).

3. Results

3.1. S-index Distributions

Figure 1 shows distributions of *S*-index values for three stellar samples introduced in Section 2.1. Not surprisingly, the short-periodic sample appears to be on average more active than the sample of solar-type stars. Interestingly, Figure 1 indicates that non-periodic stars are on average less active than solar-type stars. Furthermore, the difference between distributions of solar-type and non-periodic stars is similar to the difference between distributions of short-periodic and solar-type stars.

To quantify the difference between the distributions we computed the Kolmogorov–Smirnov (K-S) statistic (Hodges 1958). The K-S statistic are measured by the maximum diagonal distance between the empirical cumulative distribution functions of the two samples. The statistic is 0.21 for distributions between short-periodic and solar-type sample, while it is 0.27 for distributions between solar-type and non-periodic sample. The K-S statistic values and the two low *p*-values ($<10^{-6}$) indicate distributions of both sample sets are different, and distributions between the solar-type and non-periodic sample are much more different than those between short-periodic and solar-type sample.

Figure 1 indicates that though the *S*-index distributions of solar-type and non-periodic stars are different, there is a substantial overlap between them. This implies that stars with detectable and not-detectable rotation periods and, consequently, very different light curves can still have the same levels of the chromospheric activity. The example of two such stars, KIC 10414643 and KIC 5350635, is given in Figure 2 and their main parameters are summarized in Table 1. The photometric variation R_{var} is taken from Reinhold et al. (2020). It is calculated by defining the difference between the 5th and 95th percentile of the sorted differential flux in each Kepler quarter and then taking the median among all quarters value.

Figure 2 shows that while both stars have very similar Ca II *H* and *K* profiles and basically the same values of the *S*-index, their light curves are pretty different. The light curve of KIC 10414643, on the one hand, is highly regular and its rotation period can be easily determined. On the other hand, the amplitude of variability of KIC 5350635 is roughly five times smaller and no clear periodic signal can be seen behind the noise.

One possible explanation of such behavior is that chromospheric activity is mainly given by the overall coverage of a star by the magnetic features (see, e.g., Shapiro et al. 2014). At the same time, the photometric variability on stellar rotation timescale strongly depends on the surface distribution of magnetic features, their sizes, as well as evolution (see, e.g., Shapiro et al. 2020). In particular, recent studies have been able to reveal the temporal evolution of starspots (see, e.g., Namekata et al. 2020) and also determine their sizes (see, e.g., Morris et al. 2017, who showed that spots of HAT-P-11 and of the Sun have similar sizes).

One interesting effect capable of a strong increase of the photometric variability without a direct influence on the *S*-index values and, thus, explaining the difference between periodic and non-periodic stars is nesting in the distribution of magnetic features (i.e., the tendency of magnetic features to emerge within certain "nests" of activity; see, e.g., Castenmiller et al. 1986). In contrast to the spatially random distribution of emergences, nesting would lead to a non-axisymmetric distribution of spots (see, e.g., Isık et al. 2018) and, consequently, regular light curves with large amplitudes of the rotational brightness variability. The effect of nesting on the photometric variability will be addressed in the forthcoming study.[7]

Another contributing factor might be the stellar inclination, i.e., the angle between the direction to the observer and stellar rotation axis. While photometric variability and period detectability strongly depends on the inclination of a star (Nèmec et al. 2020), chromospheric activity shows a much weaker dependence (Shapiro et al. 2014). In particular, if a star is observed at a relatively low inclination (i.e., pole-on) its rotational variability would be significantly reduced and a star will be classified as non-periodic despite a large chromospheric activity. Finally, we cannot fully exclude a possible change of the *S*-index between periods of Kepler and LAMOST observations (although, see the discussion in Section 2.2). We emphasize here the need for the future contemporaneous spectroscopic and photometric observations for a large sample of stars.

3.2. Relation between S-index and Photometric Variability

In Figure 3 we plot the dependences of photometric variability on *S*-index for the solar-type and non-periodic samples. For the solar-type sample, the R_{var} significantly increases with *S*-index. We binned the *S*-index values into seven equidistant segments within the range 0.12–0.30 for the solar-type sample and within the range 0.1–0.3 for the non-periodic sample. The averaged R_{var} values in each bins were then calculated. The binned values show that for both samples photometric variability somehow increases with the *S*-index. The increase is, however, not particularly strong and is to a large extent hidden by the large spread of photometric variabilities the stars with the same *S*-index can have.

In agreement with Reinhold et al. (2020), Figure 3 shows that photometric variability of solar-type stars is significantly larger than that of non-periodic stars. The stars in the non-periodic sample exhibit variabilities similar to that of the Sun (for which median R_{var} over the last 140 yr was 0.07% and maximum R_{var} was about 0.2%; see Reinhold et al. 2020 for detailed discussion). At the same time, Figure 3 demonstrates that although distributions of *S*-index values for the periodic

[7] E. Isik (2020, private communication).

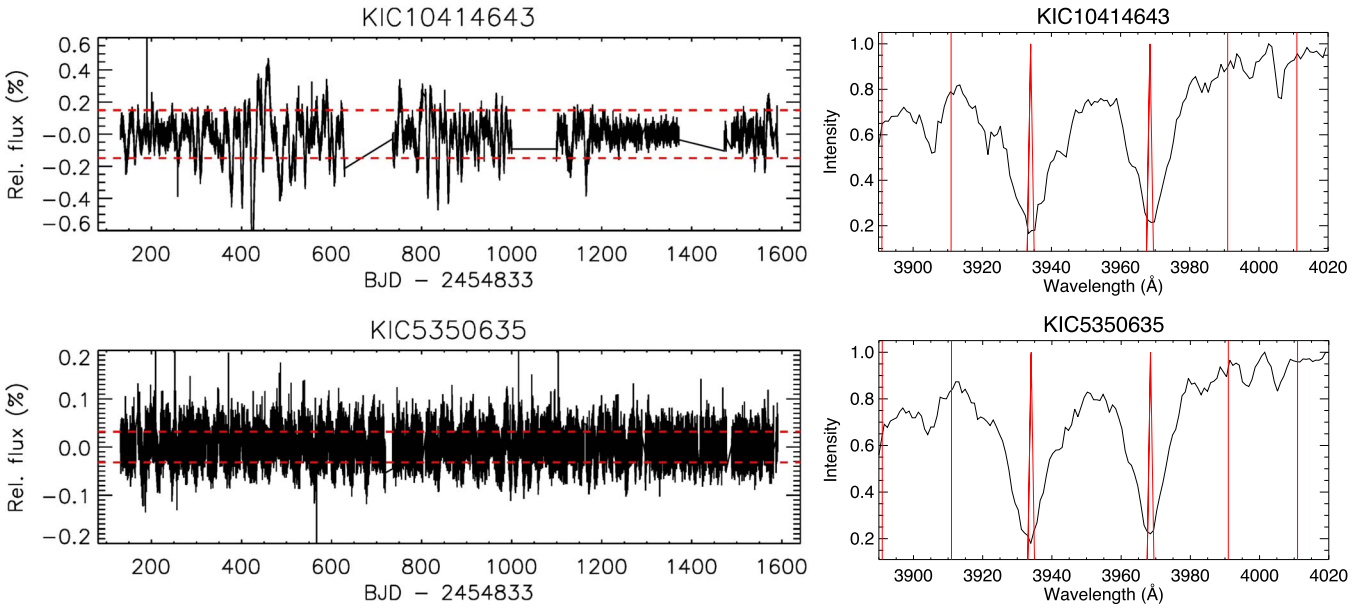

Figure 2. Kepler light curves (left panels) and LAMOST Ca II *H* and *K* profiles (right panels) for solar-type star KIC 10414643 (top panels) and non-periodic star KIC 5350635 (bottom panels), respectively. The horizontal red dashed lines in the two left panels indicate the variability range $R_{\rm var}$. The red triangles in the two right panels indicate the measurement bandpasses at the cores of Ca II *H* and *K* lines, the red rectangles indicate the measurement bandpasses of pseudo-continuum.

and non-periodic stars are different (see Section 3.1), the *S*-index is not the main factor that defines the morphology of the light curves (regular versus non-regular) and their amplitude. We note that the *S*-index mainly depends on the total coverage of stellar surface by magnetic features, while the photometric variability additionally depends on the degree of axisymmetry of this distribution (see Section 3.1). Consequently, our result hints that the surface distribution of magnetic features and its degree of axisymmetry plays an important role in defining whether a star is solar-type or non-periodic stars.

Kepler data shows that photometric variability increases with the stellar rotation rate until periods of about 12 days and saturates for faster rotators (see, e.g., Figure 15 in Notsu et al. 2019). Interestingly, the saturation appears to be less pronounced for the *S*-index values (see Figure 6 in Zhang et al. 2020). We further illustrate this point in the Appendix where we repeat Figures 1 and 3 but for samples of stars with rotational periods $P_{\rm rot} < 8$ days, $8 < P_{\rm rot} < 12$ days, $12 < P_{\rm rot} < 20$ days, and $20 < P_{\rm rot} < 30$ days (see Figures A1 and A2). One can see that *S*-index values and photometric variabilities for the last three samples are clearly different, increasing from slower to faster rotators (see red, blue, and maroon in Figures A1 and A2). For the *S*-index the same trend is also valid for stars with $P_{\rm rot} < 8$ days—they appear to be more active than stars in other samples (see yellow in Figure 1). At the same time there seems to be a saturation in the photometric variabilities as their average values for stars with $P_{\rm rot} < 8$ days and for stars with $8 < P_{\rm rot} < 12$ days are very similar (see maroon and yellow in Figure A2). This is consistent with the results of Notsu et al. (2019) and Zhang et al. (2020).

3.3. Effect of Spectral Resolution on the S-index and Placing the Sun among Solar-type Stars

The main difficulty in finding the solar *S*-index as it would be measured by LAMOST is the relatively low spectral resolution of LAMOST. Although the mean resolution power of LAMOST is about 1800, the resolution strongly depends on wavelength and is expected to be about 1000 around Ca II *H* and *K* lines (Xiang et al. 2015). Furthermore, Xiang et al. (2015) reported that the resolution power of each LAMOST fiber varies considerably, with amplitudes amounting to 1 Å. Potentially such a spread of resolutions might affect not only placing the Sun on the LAMOST *S*-index scale, but also the distributions plotted in Figure 1. Indeed, one might expect that stars with near-solar activity levels observed at lower spectral resolution will have higher *S*-index values than stars observed at higher resolution (as the lower the spectral resolution is the stronger the line cores are mixed with wings and, consequently, the larger are the *H* and *K* fluxes, see Equation (1)).

To clarify the strength of the impact of the differences in the resolution power between different LAMOST fibers on the distribution of *S*-index values, we collected the observational resolution curves at the blue end (3700–5900 Å) of the individual spectra that were obtained utilizing the LAMOST arc lamp and sky emission lines.[8] In the left panel of Figure 4 we show the dependence of the *S*-index on the LAMOST observational resolution power, i.e., FWHM for stars from Figure 1. Note that the observational resolution curves are available for ∼50% of stars in Figure 1. One can see that the dependence (if any) of the *S*-index on the LAMOST spectral resolution is rather weak compared to the differences of *S*-index values between the periodic and non-periodic sample. Consequently, we do not expect that any of our results might be affected by the LAMOST stars being observed at slightly different spectral resolutions.

It is important to place the Sun and solar-type stars on the same *S*-index scale for comparing their chromospheric activities. This, however, is hindered by the fact that LAMOST survey has no record of spectra of solar light reflected from minor bodies or from inactive satellites. Therefore, we take the following indirect approach to obtain the *S*-index of the Sun on LAMOST scale. We use the high-resolution (better than

[8] M.-S. Xiang (2020, private communication).

Table 1
Parameters of KIC 10414643 and KIC 5350635

KIC	$T_{\rm eff}$	$\log g$	[Fe/H]	$R_{\rm var}$	S-index	$P_{\rm rot}$
10414643	5692.39 ± 30.79	4.50 ± 0.05	0.02 ± 0.03	0.2991	0.2018	22.21
5350635	5829.83 ± 23.08	4.46 ± 0.04	−0.11 ± 0.02	0.0638	0.2019	

Note. The values of effective temperature, surface gravity, and metallicity are take from DR6 of the LAMOST survey. The values of photometric variations are taken from Reinhold et al. (2020). The value of rotation period is taken from McQuillan et al. (2014).

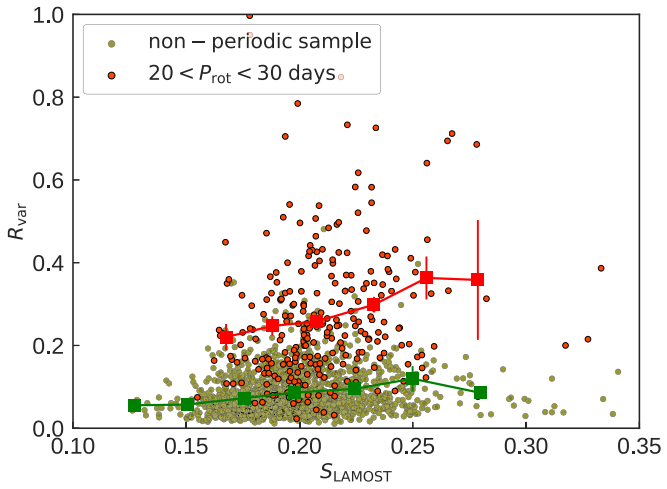

Figure 3. Dependence of photometric variability, $R_{\rm var}$, on S-index for the solar-type sample (red) and non-periodic sample (green). The red and green square symbols connected with lines represent the averaged $R_{\rm var}$ and S-index values in seven bins (see Section 3.2 for more details) for the solar-type sample and non-periodic sample, respectively. The vertical line segments indicate standard deviation of $R_{\rm var}$ values within the bin.

350,000) solar flux spectrum from Hamburg atlas[9] (see, e.g., Doerr et al. 2016) created using the data from the Fourier Transform Spectrometer (FTS) at the McMath-Pierce solar telescope at the Kitt Peak National Observatory. We degrade this FTS spectrum by convolving it with Gaussian kernels of varying FWHM in the range 0–5 Å, which covers the range of spectral resolutions achieved from LAMOST fibers. Then we compute the S-index for the high-resolution (undegraded) and degraded spectra. In the right panel of Figure 4 we show the ratio of S-index measured for the degraded spectrum to that measured for the original high-resolution FTS spectrum as a function of the resolution. Due to the increased H and K fluxes resulting from the lower spectral resolution, the ratio increases with decreasing resolution. In the left panel of Figure 4, it appears that the majority of LAMOST stars considered for this plot were observed with spectral resolution between 3.0 and 3.2 Å. For this range of resolution, the ratio varies only slightly, i.e., between 1.45 and 1.49 as indicated by the shaded horizontal bar in the right panel of Figure 4, reinforcing that S-index has a weaker dependence on the variations in LAMOST resolution. However, we note that S-index measured with a low-resolution spectra like LAMOST would be on an average larger by 47% than that measured with the high-resolution spectrum.

Egeland et al. (2017) has accurately placed the solar S-index value on the MWO S-index scale. They found that minimum and maximum values of the solar S-index during cycles 15–24 were 0.162 and 0.177, respectively. We note that these values correspond to $\alpha = 19.2$ instead of $\alpha = 14.4$ that we adopted here following Karoff et al. (2016). Thus, we first corrected Egeland et al. (2017) values for the difference in calibration factors and then applied factor 1.47 (see the right panel of Figure 4) to correct for LAMOST spectral resolution. As a result we find that solar S-index on the LAMOST scale varied between 0.179 and 0.194 during cycles 15–24. These values are designated by the dashed vertical lines in Figure 1. Compared to the activity level of the Sun, the peak level of activity of the non-periodic stars is near the range of the Sun, while the majority of the periodic stars have activity levels that are higher than that of the Sun. Consequently, the analysis of the Ca II H and K data reinforces the conclusion of Reinhold et al. (2020; drawn from the analysis of the Kepler light curves) that the Sun is a typical star of the non-periodic sample.

4. Conclusions

We derived the chromospheric activity indexes of 2603 stars in LAMOST-Kepler project. These stars were classified into three different samples. The solar-type sample includes stars with known rotation periods in range of 20–30 days, the short-periodic sample includes stars with known rotation periods in range of 10–20 days, and the non-periodic sample includes stars with unknown rotation periods. We investigated the S-index distributions of these samples. We studied the dependence of the photometric variation on the chromospheric activity level for the solar-type sample and non-periodic sample. By convolving the high-resolution solar spectrum to the LAMOST resolution, we could place the Sun on the LAMOST S-index scale.

We showed that the solar S-index values are typical for the non-periodic Kepler stars. In contrast, the stars in the solar-type sample are systematically more active than the non-periodic stars in both chromospheric activity levels and amplitudes of photometric variation. At the same time we found that non-periodic and solar-type stars can have the same values of the S-index. Consequently, the S-index, which mainly determines the total coverage of stellar surface by magnetic features, is not the main factor determining stellar photometric variability. We suggest that the surface distribution of magnetic features and, in particular, the degree of its axisymmetry, plays at least as important role in defining stellar photometric variability as the total coverage of a star by magnetic features.

This work is supported by the Joint Research Fund in Astronomy (U1631236) under cooperative agreement between the National Natural Science Foundation of China (NSFC) and Chinese Academy of Sciences (CAS), and grants 11903044 from the NSFC. S.A.I. and R.T. have been funded by the European Research Council (ERC) under the European Unions Horizon 2020 research and innovation programme (grant agreement No. 715947). X.M.-S. acknowledges support from NSFC grant No.11703035. S.K. received funding from the

[9] ftp://ftp.hs.uni-hamburg.de/pub/outgoing/FTS-Atlas/

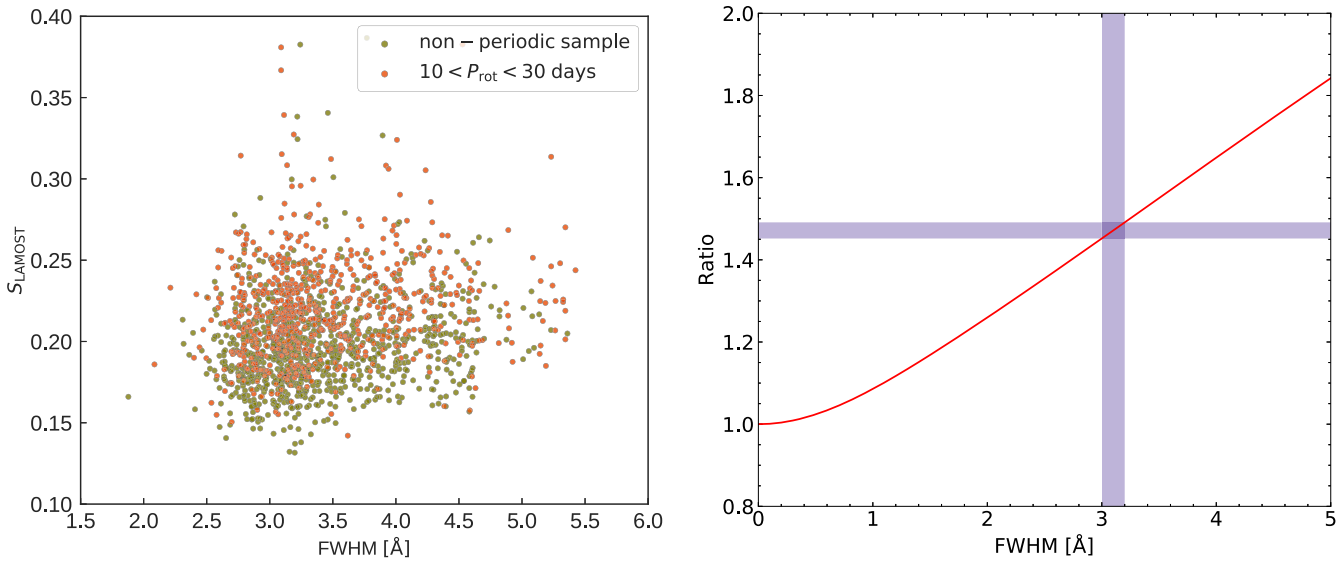

Figure 4. Left panel: the *S*-index values determined from the LAMOST spectra vs. spectral resolution power of fibers used to obtain these spectra. Right panel: modeled ratio between solar *S*-index calculated from the FTS solar spectrum convolved with Gaussian kernel of corresponding FWHM and *S*-index calculated with FTS spectrum without any convolution. The vertical shaded area in the right panel indicates the FWHM in range 3.0–3.2, where most stars from our samples were observed. The horizontal shaded area indicates the corresponding ratio in range 1.45–1.49.

European Union's Horizon 2020 research and innovation programme under the Marie Skłodowska-Curie grant agreement No. 797715. T.L. acknowledge the funding from the European Research Council (ERC) under the European Unions Horizon 2020 research and innovation programme (CartographY GA. 804752). Z.X.-F. acknowledges support from NSFC grant No. 11703001. We acknowledge the entire Kepler team and everyone involved in the Kepler mission. Funding for the Kepler Mission is provided by NASAs Science Mission Directorate. Guoshoujing Telescope (the Large Sky Area Multi-Object Fiber Spectroscopic Telescope (LAMOST)) is a National Major Scientific Project built by the Chinese Academy of Sciences. Funding for the project has been provided by the National Development and Reform Commission. LAMOST is operated and managed by the National Astronomical Observatories, Chinese Academy of Sciences.

Appendix

Distributions of S-index values (Figure A1) and the dependence of photometric variability Rvar on S-index (Figure A2) for periodic stars grouped according to their rotation periods.

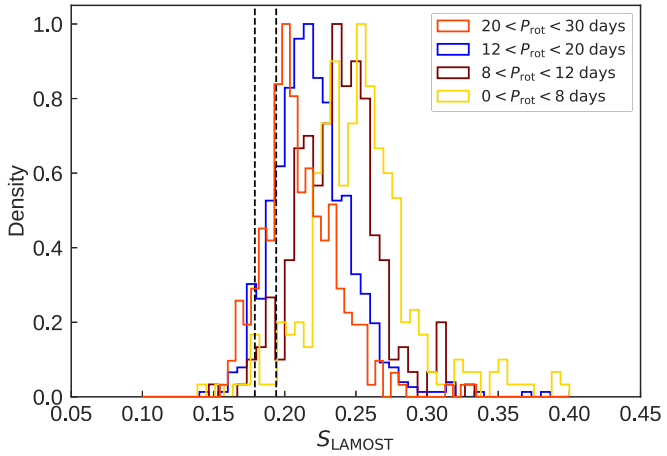

Figure A1. The same as Figure 1 from the main text but for different samples of stars (see the figure legend).

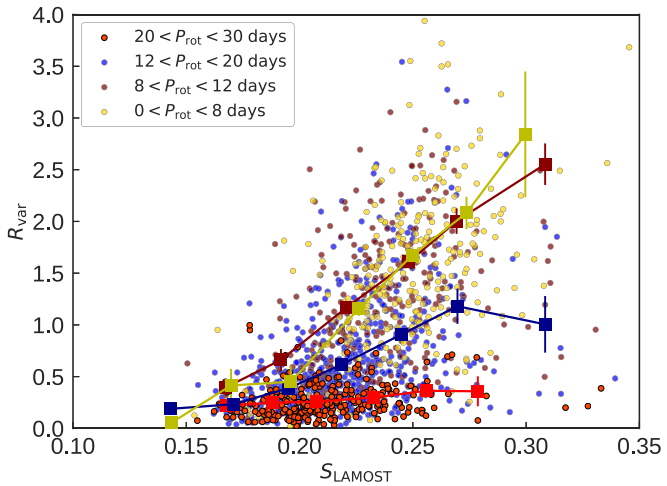

Figure A2. The same as Figure 3 from the main text but for different samples of stars (the samples shown here are the same as in Figure A1, see the figure legend).

ORCID iDs

Jinghua Zhang https://orcid.org/0000-0002-2510-6931
Shaolan Bi https://orcid.org/0000-0002-7642-7583
Maosheng Xiang https://orcid.org/0000-0002-5818-8769
Timo Reinhold https://orcid.org/0000-0002-1299-1994
Krishnamurthy Sowmya https://orcid.org/0000-0002-3243-1230

References

Aigrain, S., Llama, J., Ceillier, T., et al. 2015, MNRAS, 450, 3211
Baliunas, S. L., Donahue, R. A., Soon, W. H., et al. 1995, ApJ, 438, 269
Basri, G., Walkowicz, L. M., & Reiners, A. 2013, ApJ, 769, 37
Castenmiller, M. J. M., Zwaan, C., & van der Zalm, E. B. J. 1986, SoPh, 105, 237
Charbonneau, P. 2010, LRSP, 7, 3
Charbonneau, P. 2013, Saas-Fee Advanced Course 39, Solar and Stellar Dynamos (Berlin: Springer)
Cui, X.-Q., Zhao, Y.-H., Chu, Y.-Q., et al. 2012, RAA, 12, 1197
De Cat, P., Fu, J. N., Ren, A. B., et al. 2015, ApJS, 220, 19
Doerr, H. P., Vitas, N., & Fabbian, D. 2016, A&A, 590, A118
Egeland, R. 2017, PhD thesis, Montana State Univ.
Egeland, R., Soon, W., Baliunas, S., et al. 2017, ApJ, 835, 25
Gilliland, R. L., Chaplin, W. J., Dunham, E. W., et al. 2011, ApJS, 197, 6
Hall, J. C., Henry, G. W., Lockwood, G. W., Skiff, B. A., & Saar, S. H. 2009, AJ, 138, 312
Hall, J. C., Lockwood, G. W., & Skiff, B. A. 2007, AJ, 133, 862
Hodges, J. L. 1958, ArM, 3, 469
Isaacson, H., & Fischer, D. 2010, ApJ, 725, 875
Isık, E., Solanki, S. K., Krivova, N. A., & Shapiro, A. I. 2018, A&A, 620, A177
Karoff, C., Knudsen, M. F., De Cat, P., et al. 2016, NatCo, 7, 11058
Lockwood, G. W., Skiff, B. A., Henry, G. W., et al. 2007, ApJS, 171, 260
Luo, A. L., Zhao, Y.-H., Zhao, G., et al. 2015, RAA, 15, 1095
McQuillan, A., Mazeh, T., & Aigrain, S. 2014, ApJS, 211, 24
Morris, B. M., Hebb, L., Davenport, J. R. A., Rohn, G., & Hawley, S. L. 2017, ApJ, 846, 99
Namekata, K., Davenport, J. R. A., Morris, B. M., et al. 2020, ApJ, 891, 103
Nèmec, N. E., Shapiro, A. I., Krivova, N. A., et al. 2020, A&A, 636, A43
Notsu, Y., Maehara, H., Honda, S., et al. 2019, ApJ, 876, 58
Noyes, R. W., Hartmann, L. W., Baliunas, S. L., Duncan, D. K., & Vaughan, A. H. 1984, ApJ, 279, 763
Radick, R. R., Lockwood, G. W., Henry, G. W., Hall, J. C., & Pevtsov, A. A. 2018, ApJ, 855, 75
Radick, R. R., Lockwood, G. W., Skiff, B. A., & Baliunas, S. L. 1998, ApJS, 118, 239
Reinhold, T., Cameron, R. H., & Gizon, L. 2017, A&A, 603, A52
Reinhold, T., Shapiro, A. I., Solanki, S. K., et al. 2020, Sci, 368, 518
Salabert, D., García, R. A., Beck, P. G., et al. 2016, A&A, 596, A31
Shapiro, A. I., Amazo-Gómez, E. M., Krivova, N. A., & Solanki, S. K. 2020, A&A, 633, A32
Shapiro, A. I., Solanki, S. K., Krivova, N. A., et al. 2014, A&A, 569, A38
Vidotto, A. A. 2019, arXiv:1911.10915
Wilson, O. C. 1978, ApJ, 226, 379
Witzke, V., Reinhold, T., Shapiro, A. I., Krivova, N. A., & Solanki, S. K. 2020, A&A, 634, L9
Witzke, V., Shapiro, A. I., Solanki, S. K., Krivova, N. A., & Schmutz, W. 2018, A&A, 619, A146
Wood, B. E. 2004, LRSP, 1, 2
Xiang, M. S., Liu, X. W., Yuan, H. B., et al. 2015, MNRAS, 448, 822
Zhang, J., Bi, S., Li, Y., et al. 2020, ApJS, 247, 9
Zhao, G., Zhao, Y.-H., Chu, Y.-Q., Jing, Y.-P., & Deng, L.-C. 2012, RAA, 12, 723
Zong, W., Fu, J.-N., De Cat, P., et al. 2018, ApJS, 238, 30